CrystEngComm

RSC Publishing

PAPER

View Article Online
View Journal | View Issue

Cite this: *CrystEngComm*, 2013, **15**, 10100

A synthesis and up-conversional photoluminescence study of hexagonal phase $NaYF_4$:Yb,Er nanoparticles

ShiYong Yu, XueChuan Gao, Hui Jing, Jing Zhao and Haiquan Su*

Received 15th September 2013,
Accepted 5th October 2013

DOI: 10.1039/c3ce41857j

www.rsc.org/crystengcomm

In this article, hexagonal phase $NaYF_4$:Yb,Er (β-$NaYF_4$:Yb,Er) nanoparticles with a controlled size and morphology were synthesized *via* a simple and environmentally friendly method under relatively mild conditions. The different F^-/Y^{3+} molar ratios were used in the synthesis of hexagonal Yb^{3+},Er^{3+} codoped $NaYF_4$ nanocrystals as a means of controlling the size and morphology of the nanocrystals. Subsequently, the morphology and structure of the products were characterized by transmission electron microscopy (TEM) and X-ray diffraction (XRD). The effect of the F^-/Y^{3+} molar ratio on the size and morphology of the products was examined. When the F^-/Y^{3+} molar ratio was gradually increased, the products transformed from spherical hexagonal nanocrystals to regular hexagonal nanocrystals and the size of the products changed from 8 to 400 nm. That is to say, excessive F^- ions were capable of accelerating for the formation of larger β-$NaYF_4$:Yb,Er nanoparticles in our synthesis procedure. Meanwhile the upconversion photoluminescence of the nanocrystals was investigated in detail by fluorescent spectroscopy to reveal the relationship between the optical properties and the morphology and size of the products. As a consequence, the upconversion photoluminescence of the nanocrystals demonstrated a morphology and size dependence. Thus the fabrication of β-$NaYF_4$:Yb,Er nanoparticles with different sizes and morphologies would satisfy the diverse requirements in various fields.

Introduction

It is well known that upconversion is an anti-Stokes process in which long wavelength radiation, usually near-infrared radiation, is converted to short wavelength radiation such as visible or ultraviolet radiation.[1–3] Thus upconversion materials, as an important family of inorganic biomaterials, have attracted much attention for their potential applications in biomedical and biotechnological fields due to this unique property. Compared with the conventional downconversion inorganic fluorophores,[4] organic dyes[5] and semiconductor quantum dots,[6] upconversion luminescent materials can emit higher-energy visible photons after being excited by lower-energy near-infrared photons.[7] The near-infrared excitation allows a deeper penetration in biological tissues and has a weaker autofluorescence because the UV-excitable biological tissues and fluorescent drug molecules that interfered with the normal phosphor luminescence can no longer be excited by near-infrared radiation,[8] which brings many advantages over organic dye markers and quantum dots for biological applications. In addition, upconversion luminescent nanomaterials have been widely studied in various optical devices such as solid-state lasers, three-dimensional flat-panel displays, and low-intensity IR imaging.[9–12]

As we know that the shape and size of nanocrystals have a crucial influence on their physical and chemical properties, which, in turn, determine their applications.[13,14] For example, for biological applications, the upconversion luminescent nanomaterials need not only to be less than 20 nm, but also to be spherically shaped whilst maintaining a high degree of biocompatibility and monodispersion.[15,16] When they are applied in optical fields, an excellent crystalline structure and strong upconversion luminescence will be requirement. Therefore, it is significant to synthesize upconversion luminescent nanomaterials with a controlled shape and size to meet the various requirements in different fields.

Among various upconversion luminescent nanomaterials, hexagonal phase rare earth ion-Yb,Er codoped $NaYF_4$, which is known as one of the most efficient upconversion luminescent nanomaterials under near-infrared excitation, has attracted more and more attention. It is widely known that $NaYF_4$ has been used as one of the most efficient hosts for upconversion rare earth ions. The crystal structures of $NaYF_4$ belong to the cubic (α-$NaYF_4$) or hexagonal (β-$NaYF_4$) phase. The hexagonal phase is thermodynamically stable, whereas the cubic phase is high-temperature metastable. In addition, the hexagonal phase $NaYF_4$:Yb,Er crystal exhibits a higher fluorescence efficiency than the cubic phase $NaYF_4$:Yb,Er crystal.[17] The Er^{3+} ion has been widely recognized as one of

Inner Mongolia Key Laboratory of Chemistry and Physics of Rare Earth Materials, School of Chemistry and Chemical Engineering, Inner Mongolia University, Inner Mongolia, Hohhot 010021, China. E-mail: haiquansu@yahoo.com; Tel: +976 0471 4992981

the most suitable upconversion rare earth ions to convert infrared to visible light. This is because it possesses a favourable electronic energy level scheme that can be accessed under near infrared radiation. The Yb^{3+} ions can remarkably enhance the upconversion efficiency from infrared to visible due to the efficiency of the energy transfer from Yb^{3+} to Er^{3+}. Therefore, the fabrication of pure, hexagonal-system $NaYF_4$:Yb,Er nanocrystals with various sizes and morphologies by facile routes are very important.

Up to now, a vast amount of studies have investigated the synthesis of hexagonal-system $NaYF_4$:Yb,Er nanocrystals using different methods. For example solvothermal,[18] hydrothermal methods,[19]co-precipitation methods,[20] microwave-assisted synthesis[21] and so on. However, these techniques are always complicated and have low crystallinities, high costs and environmental loads. Therefore it is essential to find a simple, high crystallinity, low cost, and environmentally friendly method to prepare hexagonal phase $NaYF_4$:Yb, Er nanomaterials. Herein we report a thermal decomposition procedure with considerably mild conditions and a shortened time for achieving simultaneous control over the size, morphology and luminescence properties of β-$NaYF_4$:Yb,Er by just using different F^-/Y^{3+} molar ratios. β-$NaYF_4$:Yb^{3+},Er^{3+} nanocrystals with a controlled size and shape are synthesized successfully by tuning the F^-/Y^{3+} molar ratio. The upconversion emission properties of the resultant β-$NaYF_4$:Yb,Er nanocrystals are also characterized.

Experimental

Chemicals

The synthesis was carried out using standard oxygen-free procedures and commercially available reagents. Deionized water was used throughout. $Y(NO_3)_3{\cdot}6H_2O$, $Er(NO_3)_3{\cdot}6H_2O$, $Yb(NO_3)_3{\cdot}6H_2O$, NaOH, sodium stearate, cyclohexane, ethanol, oleic acid, oleylamine, 1-octadecene and hydrofluoric acid were of analytical grade and used as received without further purification.

The synthesis of β-phase $NaYF_4$:Yb^{3+},Er^{3+}

All the β-phase $NaYF_4$:Yb^{3+},Er^{3+} nanocrystals were prepared *via* thermal decomposition under relatively mild synthetic conditions. This process generally consisted of the following three parts.

The synthesis of rare-earth oleate

Firstly, a transparent aqueous solution of $Y(NO_3)_3$, $Yb(NO_3)_3$ and $Er(NO_3)_3$ (lanthanide ion molar ratio, Y/Yb/Er = 0.8/0.15/0.05) was mixed with a milky solution which was prepared by mixing 0.36 g NaOH, 3 ml oleic acid, 4 ml ethanol and 6 ml of cyclohexane under vigorous stirring, to result in a white mixture. The white mixture was then transferred into a 50 ml autoclave and treated at 80 °C for 4 h. Subsequently, it was cooled down to room temperature naturally. Finally, the obtained rare-earth oleate in the oil layer was collected and diluted to 20 ml with cyclohexane.

The synthesis of hydrofluoric acid/oleylamine mixture

The mixture was achieved by dissolving 3 ml HF into 17 ml oleylamine, and subsequently 3 ml of cyclohexane and 7 ml of ethanol were introduced. Then the mixture was stirred for 30 min and formed an optically transparent solution. The solution was stored at room temperature for further use.

The synthesis of β-phase $NaYF_4$:Yb^{3+},Er^{3+} with different sizes and sharps

Firstly, 12 ml oleic acid, 3 ml 1-octadecene and 0.35 g sodium stearate were added into a three necked flask at room temperature. Next 4 ml as-prepared rare-earth oleate solution and 1.2 ml of the aforementioned HF–oleylamine solution (F^-/Y^{3+} = 1.2/4) were added into the three necked flask when the mixture was heated to 80 °C under vigorous stirring. After that the solution was kept at 80 °C for 20 min. Then it was heated to 180 °C and kept at this temperature for 10 min. Subsequently it was heated to 310 °C and kept at this temperature for 1 h and then cooled down to room temperature naturally. The reaction mixture was kept under a protective nitrogen flow and was well stirred throughout. The obtained β-$NaYF_4$:Yb,Er nanocrystals were collected and washed several times with cyclohexane and absolute ethanol in turn. Finally, the products were dried in air at about 70 °C.

Then the above synthetic procedure was used to synthesize β-$NaYF_4$:Yb,Er nanocrystals with F^-/Y^{3+} = 1.4/4, 1.6/4, 2.0/4. The F^-/Y^{3+} = 1.2/4, 1.4/4, 1.6/4 and 2.0/4 were referred to as samples a, b, c and d, respectively.

Measurement and characterization

The crystallinity of β-$NaYF_4$:Yb,Er was analyzed by a PANalytical Empyrean sharp shadow system X-ray diffractometer (XRD) at a scanning rate of 2° min^{-1} in 2θ range from 10° to 80° which employed Cu Kα radiation (λ = 1.540598 Å). The operating current and voltage were kept at 55 mA and 60 kV, respectively. The size and morphology of the β-$NaYF_4$:Yb,Er were inspected using a FEI Tecnai HRTEM (G^2 F20). A small drop of the sample dispersed in ethanol was deposited on a Cu grid and dried for the TEM measurement in air. Energy dispersive X-ray (EDX) analysis was carried out on a transmission electron microscope (FEI DPP-II). Photoluminescence (PL) spectra was performed on an Edinburgh Instruments FLS920 spectrophotometer equipped with a 980 nm laser as the excitation source. Fourier transform infrared spectroscopy (FTIR) spectra was recorded with a NEXUS-670 Fourier-transform infrared spectrophotometer. The sample was mixed with potassium bromide at 1/10 weight ratio. All measurements were performed at room temperature.

Results and discussions

Fig. 1 shows the XRD pattern of the as-prepared $NaYF_4$:Yb^{3+}, Er^{3+}. The peak positions and intensities of the nanocrystal were in good agreement with the data in (JCPDS 28-1192), indicating that the obtained $NaYF_4$:Yb^{3+},Er^{3+} was the hexagonal phase. Also, the sharp diffraction peaks proved that the obtained products were well crystallized, which is consistent with the TEM results. It is worth noting that there was no second phase found in the XRD measurements, indicating that the Er^{3+}, Yb^{3+} ions were effectively doped into the host lattice of β-NaYF4.

The TEM images of the obtained β-$NaYF_4$:Yb,Er nanoparticles prepared with different F^-/Y^{3+} molar ratios are displayed in Fig. 2. It was observed clearly that the upconversion hexagonal phase $NaYF_4$:Yb,Er nanoparticles with different F^-/Y^{3+} molar ratios presented different morphologies and sizes. When the F^-/Y^{3+} molar ratio was increased from 1.2/4 to 2.0/4, the size of the nanoparticles changed from 8 to 400 nm, and simultaneously, the morphology changed from spherical hexagonal nanoparticles to irregular hexagonal nanoparticles and ultimately to regular hexagonal nanoparticles. The β-$NaYF_4$:Yb,Er nanocrystals grown at 1.2/4 (F^-/Y^{3+} molar ratio) tended to grow into homogeneous nanospheres of 8 nm in diameter as shown in Fig. 2(a). When the F^-/Y^{3+} molar ratio was increased to 1.4/4, the obtained products were a rounded-like shape with an average diameter of 10 nm as shown in Fig. 2(b). When the F^-/Y^{3+} molar ratio gradually increased to 1.6/4, the obtained crystals exhibited an irregular hexagonal phase with a diameter of 20–25 nm as shown in Fig. 2(c). When the F^-/Y^{3+} molar ratio was further increased to 2.0/4 the shape evolved from an irregular hexagonal phase into a regular hexagonal phase as shown in Fig. 2(d). The diameter of the regular hexagonal $NaYF_4$:Yb,Er nanocrystals was about 400 nm. Fig. 2(e) depicts a high-resolution TEM image of the obtained $NaYF_4$:Yb,Er, with the arrows indicating that the lattice spacings were 0.355 nm and 0.516 nm, which correspond to the {001} and {100} planes, respectively, of β-phase $NaYF_4$. The fast Fourier transform diffraction pattern is shown in the inset of Fig. 2(e), which also confirmed the hexagonal phase of the products. The EDS spectra indicated that fluorine, sodium, ytterbium, erbium and yttrium atoms were detected in the obtained crystals in Fig. 2(f). In addition, there was no aggregation of all of the obtained particles, indicating a good dispersion of the nanocrystals which thus facilitates their applications in various fields.

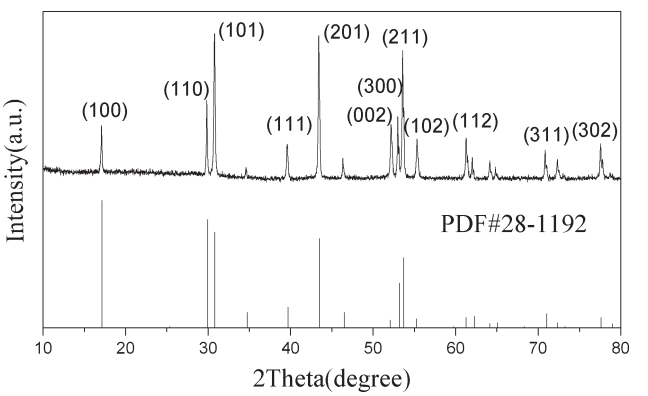

Fig. 1 The XRD power pattern of the obtained hexagonal phase $NaYF_4$:Yb^{3+},Er^{3+} and the standard XRD pattern of hexagonal phase $NaYF_4$:Yb^{3+},Er^{3+} whose PDF number is 28-1192.

It is well known that, in the synthesis of $NaYF_4$:Yb,Er, F^- acted as both a reactant and a mineralizer and that it was used to adjust the size and morphology of the $NaYF_4$:Yb,Er nanocrystals.[22] The size and morphology of β-phase $NaYF_4$:Yb,Er were found to be decided by the F^-/Y^{3+} molar ratio in our synthesis procedure, which in turn provided the feasibility of controlling the size and morphology. Spherical hexagonal nanoparticles with high upconversion luminescence efficiencies were acquired with the lower F^-/Y^{3+} molar ratio, which may meet the requirements of biological applications. With excessive F^- ions, regular hexagonal phase $NaYF_4$:Yb,Er was achieved successfully, and this could be applied in lighting.

The surface properties of the obtained $NaYF_4$:Yb^{3+},Er^{3+} were characterized by FTIR. The FTIR spectrum is shown in Fig. 3. The broad band at 3435 cm^{-1} is associated with the stretching band of the O–H (COO–H) group, while the strong peaks at 2964 cm^{-1} and 2854 cm^{-1} correspond to the respective asymmetric (*v*as) and symmetric (*v*s) stretching vibration of the methylene (CH_2) groups in the long alkyl chain of the oleic acid molecule. The bands at 1565 cm^{-1} and 1464 cm^{-1} are attributed to the asymmetric (*v*as) and symmetric (*v*s) stretching vibrations of the carboxylate group [(–COO–)$_3$$Ln^{3+}$] respectively.[23,24] These data are in close agreement with those of oleic acid, which confirmed that oleic acid was in fact on the nanoparticle surface. The addition of oleic acid used as the surfactant was favorable for controlling the size and shape of the hexagonal phase $NaYF_4$:Yb,Er nanocrystals.

As is well known, lanthanides are well-suited for upconversion applications because of the multiple metastable levels associated with the filling of the 4f-shell. Among the various lanthanides, Er^{3+} is commonly used as an activator which possesses the ladder-like arranged energy levels as shown in Fig. 4. The energy difference between the $^4I_{11/2}$ and $^4I_{15/2}$ levels was ~10350 cm^{-1} and that between the $^4F_{7/2}$ and $^4I_{11/2}$ levels was ~10370 cm^{-1}, which were able to generate upconversion emissions using 980 nm excitation. Also, the $^4I_{11/2}$ state could relax to the $^4I_{13/2}$ state and then it was excited to the $^4F_{9/2}$ state with a phonon-assisted energy transfer. Thus Er^{3+} is well-suited for upconversion applications.

β-$NaYF_4$ is known to be an efficient host for the upconversion process because of its low phonon energy. Yb^{3+} and Er^{3+} ions were selected as the doping ions to investigate the spectral and upconversion luminescent properties of the products. Fig. 5 presents the energy levels of the Yb^{3+} and Er^{3+} ions as well as the upconversion mechanism that had been proposed. As is well known, the upconversion efficiency of the β-$NaYF_4$ co-doped with Er^{3+} and Yb^{3+} was considerably

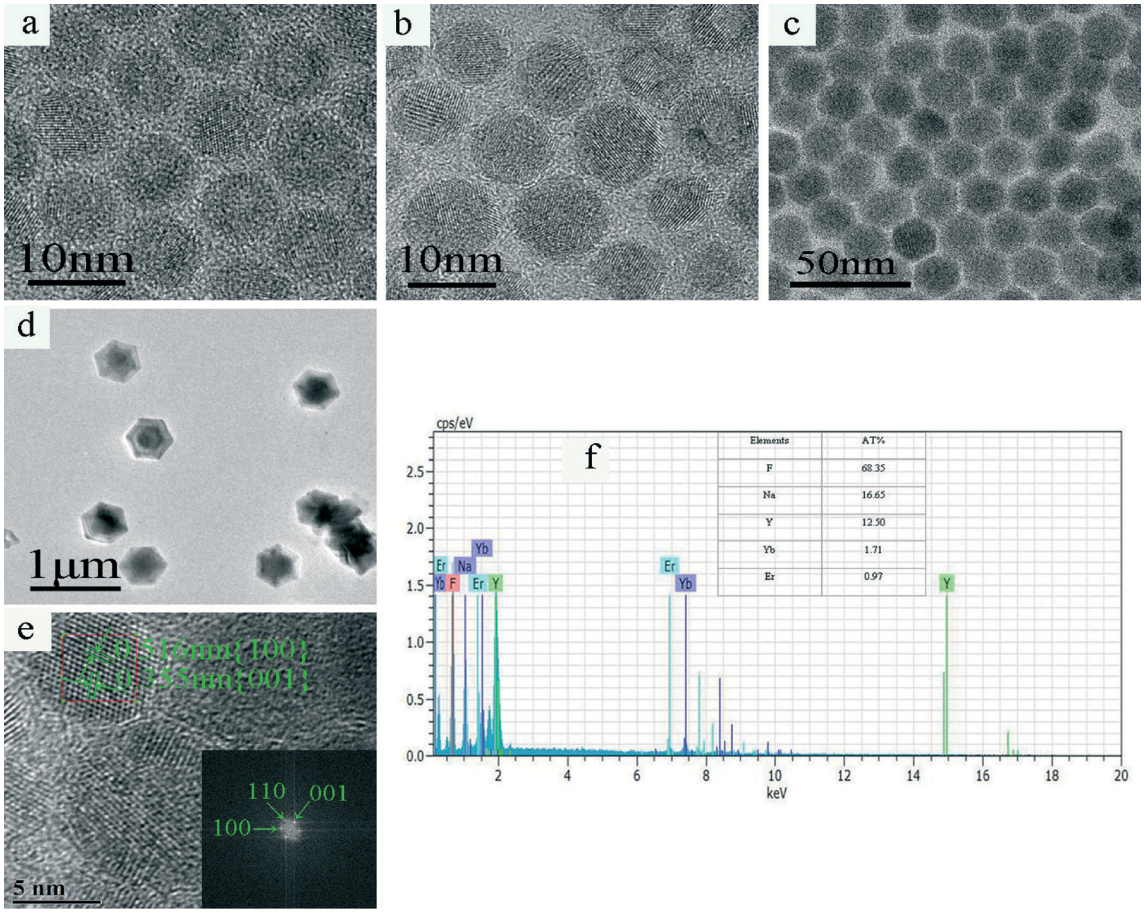

Fig. 2 (a) to (d): corresponding TEM images of the as-prepared upconversion hexagonal phase $NaYF_4$:Yb,Er nanoparticles in which F^-/Y^{3+} = 1.2/4 (a), 1.4/4 (b), 1.6/4 (c) and 2.0/4 (d), respectively. (e) A high-resolution TEM image of sample b. (f) The EDS image of the obtained sample a. The inset of (e) is the fast Fourier transform diffraction pattern.

higher than that of the β-$NaYF_4$ material doped only with Er^{3+}, which had been shown in many articles.[25] In the upconversion process, the Yb^{3+} ion absorbed one laser photon and it was excited from the $^2F_{7/2}$ state to the $^2F_{5/2}$ state. Then, Yb^{3+} that had been excited transferred its absorbed energy to the neighboring Er^{3+} ion. Subsequently, the Er^{3+} ion was excited from the $^4I_{15/2}$ to the $^4I_{11/2}$, and then to the

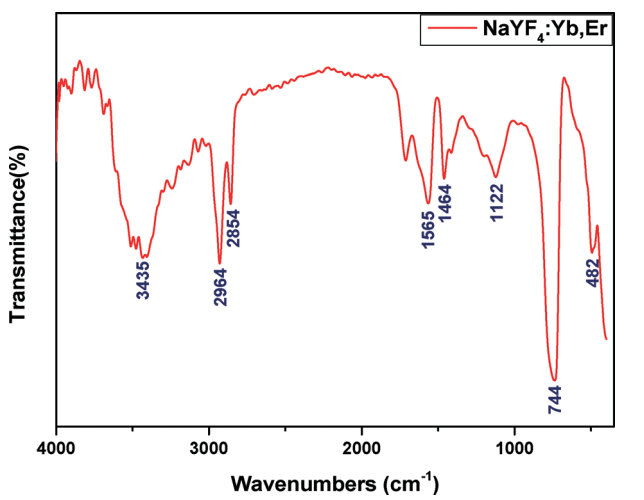

Fig. 3 The FTIR spectrum of the as-prepared upconversion hexagonal phase $NaYF_4$:Yb,Er nanoparticles.

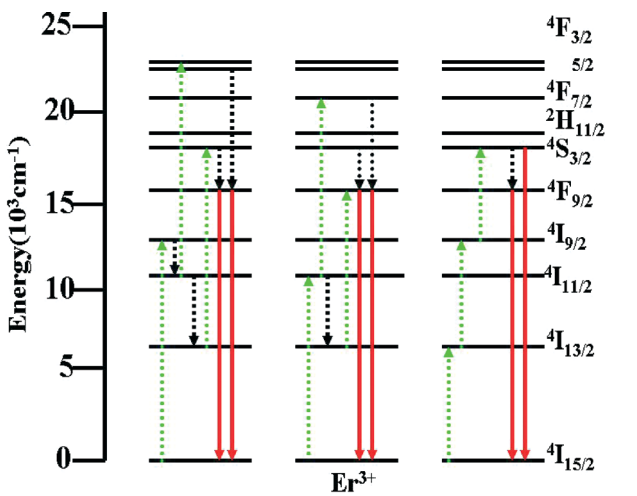

Fig. 4 The energy level diagrams of Er^{3+} and the typical upconversion process for Er^{3+}. The green dotted arrows, black dotted arrows and red full arrows represent the excitation processes, multiphonon relaxation processes and emission processes, respectively.

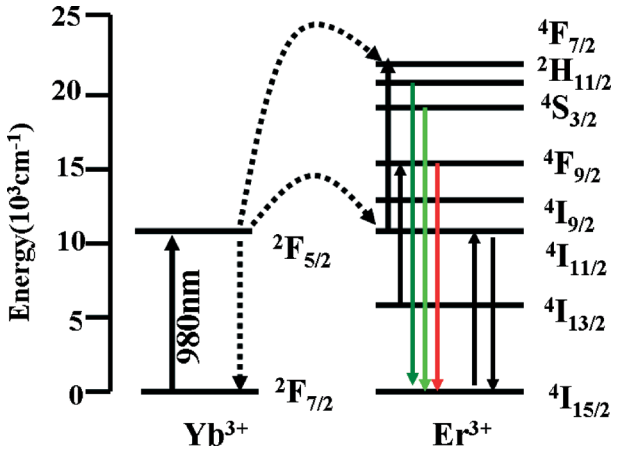

Fig. 5 The energy level diagrams of the Yb^{3+} and Er^{3+} ions and the proposed energy transfer mechanism of the upconversion processes in the Er^{3+} and Yb^{3+} co-doped crystals under 980-nm diode laser excitation. The black full arrows, black dotted arrows and colorized full arrows represent the excitation processes, energy transfer processes and emission processes, respectively.

$^4F_{7/2}$ state. Multiphonon assisted relaxations from the $^4F_{7/2}$ state could then populate the $^2H_{11/2}$ level that could generate the 521 nm emission and the $^4S_{3/2}$ level that could generate the 540 nm emission. The red emission centred at about 656 nm originated from the $^4F_{9/2} \rightarrow {}^4I_{15/2}$ transition and the $^4F_{9/2}$ state could be populated from the $^4S_{3/2}$ level based on nonradiative relaxations.

The upconversion luminescence of the hexagonal phase $NaYF_4$:Yb,Er nanoparticles prepared with different F^-/Y^{3+} molar ratios (a) 1.2/4 (b) 1.4/4 (c) 1.6/4 (d) 2.0/4 (λex = 980 nm) are depicted in Fig. 6. To make the comparison reasonable, the experimental conditions for all of the measurements were kept consistent. The three obvious emission bands centered at 526, 543, and 667 nm correspond to the $^2H_{11/2} \rightarrow {}^4I_{15/2}$ (green), $^4S_{3/2} \rightarrow {}^4I_{15/2}$ (green) and $^4F_{9/2} \rightarrow {}^4I_{15/2}$ (red) transitions of the Er^{3+} ions, respectively, which were consistent with energy transfer mechanism of the upconversion process in the Er^{3+} and Yb^{3+} co-doped crystals. It was obvious that the fluorescence intensity varied with F^-/Y^{3+} molar ratio. That is to say, the fluorescence intensity varied with the size and shape. The daylight and luminescence photos of the as-prepared $NaYF_4$:Yb,Er nanoparticles dispersed in the water solution are shown in Fig. 6e and f, respectively. The green light emission could be clearly seen by 980 nm laser irradiation (see Fig. 6f), which exhibited the excellent upconversion luminescence property of the nanocomposite. The intensity of the emissions increased with the size of the nanoparticles, which might be because the larger the size of nanoparticles was, the lower the surface defects and the stronger the emissions were. However the fluorescence intensity was not proportional to the size of the nanoparticles, which could be seen in Fig. 7. Also, the fluorescence intensity of the green emission increased dramatically with the size in comparison with that of the red emission, which indicated that the electron in the $^4I_{11/2}$ state promoted to the $^4F_{7/2}$ state may be easier than that *via* a nonradiative relaxation to the $^4I_{13/2}$ state. In addition, the crystallinities of the nanoparticles were improved which could also enhance the upconversion luminescence. Furthermore it was clearly that the calculated color coordinates ranged from (0.2753, 0.6485) to (0.3235, 0.6471) when the F^-/Y^{3+} molar ratio was changed from 1.2/4 to 2.0/4 in Fig. 8. Therefore, it was possible to achieve upconversion nanoparticles with different upconversion emissions to meet different needs.

In order to better understand the upconversion mechanism, the pump power-dependence of the green (543 nm) and red (667 nm) upconversion emissions were systematically measured and are presented in Fig. 9. According to the upconversion mechanism, the relationship between the fluorescent intensity and the pump laser power could be approximately described as $I \propto P^n$, where I is known as the fluorescent intensity, P is the pump laser power and n is the number of laser photons that were necessary to produce the upconversion emission bands.[26] Obviously, the values of the slope n were 1.53 and 1.25 corresponding to the $^4S_{3/2} \rightarrow {}^4I_{15/2}$ (green) and $^4F_{9/2} \rightarrow {}^4I_{15/2}$ (red) upconversion emissions, respectively. These values indicated that two photons were

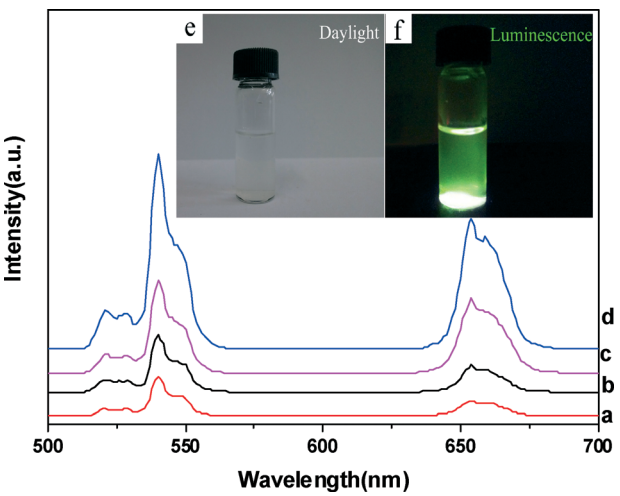

Fig. 6 The upconversion photoluminescence spectra of the hexagonal phase $NaYF_4$:Yb^{3+},Er^{3+} nanocrystals with different F^-/Y^{3+} molar ratios (a) 1.2/4 (b) 1.4/4 (c) 1.6/4 (d) 2.0/4 (λex = 980 nm). Inset: daylight (e) and luminescence (f) photos of the as-prepared $NaYF_4$:Yb,Er nanoparticles dispersed in the water solution.

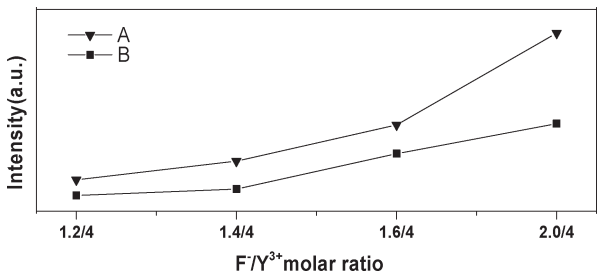

Fig. 7 The fluorescence intensity of the hexagonal phase $NaYF_4$:Yb^{3+},Er^{3+} nanocrystals centered at 543 nm (A) and 667 nm (B) with different F^-/Y^{3+} molar ratios.

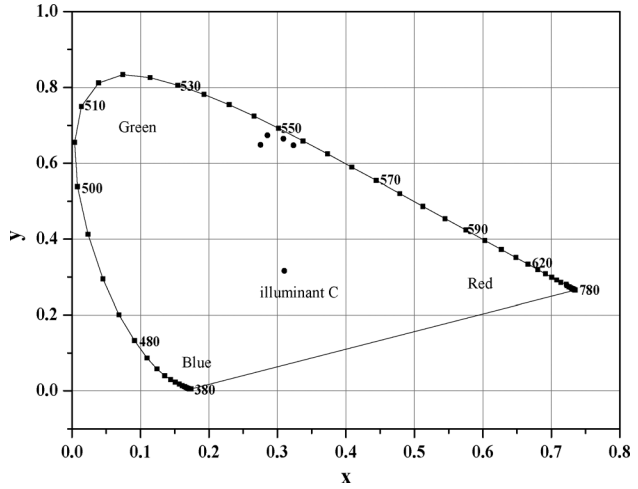

Fig. 8 The CIE chromaticity diagram of 1931 together with the calculated color coordinates in the hexagonal phase $NaYF_4$:Yb^{3+},Er^{3+} nanocrystals with different F^-/Y^{3+} molar ratios under excitation by a 980 nm laser diode.

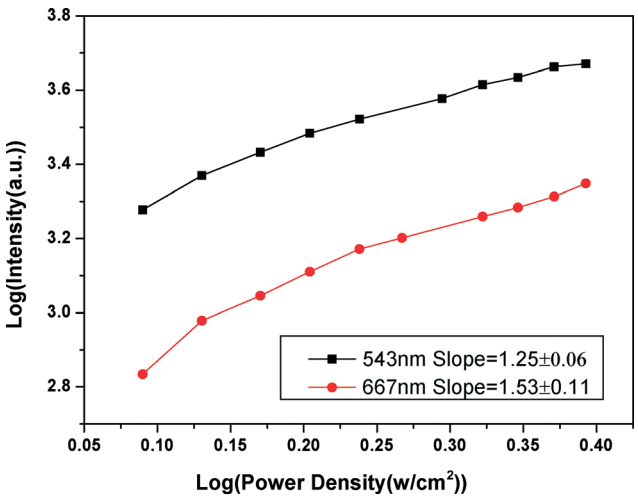

Fig. 9 The log–log plots of the upconversion emission intensity *versus* the pump-power densities in the $NaYF_4$:Yb^{3+},Er^{3+} nanocrystals under excitation by the 980 nm laser diode.

involved to produce the upconversion emission bands centered at 543 nm and 667 nm.

Conclusion

A simple and environmentally friendly thermal decomposition route under relatively mild conditions was developed successfully for the synthesis of hexagonal phase $NaYF_4$:Yb^{3+}, Er^{3+} with different morphologies and sizes. The size and morphology of the products could be easily controlled through adjusting the F^-/Y^{3+} molar ratio. Products with sizes ranging from 8 to 400 nm and morphologies evolved from spherical hexagonal nanoparticles to regular hexagonal nanoparticles have been achieved successfully. In addition, the upconversion photoluminescence of the nanocrystals was investigated in detail by fluorescent spectroscopy to reveal the relationship between the optical properties and the morphology and size of the products, and the upconversion photoluminescence of the nanocrystals demonstrated a morphology and size dependence. This work may provide a promising alternative for making upconversion luminescent hexagonal $NaYF_4$:Yb^{3+},Er^{3+} nanocrystals that meet the requirements of various applications in many fields.

Acknowledgements

The authors are grateful to the financial aid from the National Natural Science Foundation of China (grant no. 20961006), the Inner Mongolia Natural Science Foundation (grant no. 20080404MS0201), and the Inner Mongolia Technology Innovation and Guidance Funds.

References

1 (*a*) J. J. Zhou, G. X. Chen, E. Wu, G. Bi, B. T. Wu, Y. Teng, S. F. Zhou and J. R. Qiu, *Nano Lett.*, 2013, **13**, 2241; (*b*) Z. Deutsch, L. Neeman and D. Oron, *Nat. Nanotechnol.*, 2013, **8**, 649.

2 Z. Y. Cheng, R. T. Chai, P. G. Ma, Y. L. Dai, X. J. Kang, H. Z. Lian, Z. Y. Hou, C. X. Li and J. Lin, *Langmuir*, 2013, **29**, 9573.

3 Y. X. Liu, D. S. Wang, J. X. Shi, Q. Peng and Y. D. Li, *Angew. Chem., Int. Ed.*, 2013, **52**, 4366.

4 X. Qin, Y. G. Ju, S. Bernhard and N. Yao, *J. Mater. Res.*, 2005, **20**, 2960.

5 J. L. Seifert, R. E. Connor, S. A. Kushon, M. Wang and B. A. Armitage, *J. Am. Chem. Soc.*, 1999, **121**, 2987.

6 W. C. Chan and S. M. Nie, *Science*, 1998, **281**, 2016.

7 (*a*) M. Haase and H. Schäfer, *Angew. Chem., Int. Ed.*, 2011, **50**, 5808; (*b*) K. A. Abel and J. C. Boyer, *J. Am. Chem. Soc.*, 2009, **131**, 14644; (*c*) J. C. Boyer, L. A. Cuccia and J. A. Capobianco, *Nano Lett.*, 2007, **7**, 847; (*d*) N. M. Sangeetha and F. C. J. M. van Veggel, *J. Phys. Chem. C*, 2009, **113**, 14702; (*e*) H. Q. Wang and T. Nann, *ACS Nano*, 2009, **3**, 3804; (*f*) F. Wang, R. R. Deng, J. Wang, Q. X. Wang, Y. Han, H. M. Zhu, X. Y. Chen and X. G. Liu, *Nat. Mater.*, 2011, **10**, 968; (*g*) Z. Liu, L. N. Sun, F. Y. Li, Q. Liu, L. Y. Shi, D. S. Zhang, S. Yuan, T. Liu and Y. N. Qiu, *J. Mater. Chem.*, 2011, **21**, 17615.

8 (*a*) L. Y. Wang, R. X. Yan, Z. Y. Hao, L. Wang, J. H. Zeng, J. Bao, X. Wang, Q. Peng and Y. D. Li, *Angew. Chem., Int. Ed.*, 2005, **44**, 6054; (*b*) F. Zhang, G. B. Braun, Y. F. Shi, Y. C. Zhang, X. H. Sun, N. O. Reich, D. Y. Zhao and G. Stucky, *J. Am. Chem. Soc.*, 2010, **132**, 2850; (*c*) G. F. Wang, Q. Peng and Y. D. Li, *Acc. Chem. Res.*, 2011, **44**, 322; (*d*) Z. H. Xu, P. A. Ma, C. X. Li, Z. Y. Hou, X. F. Zhai, S. S. Huang and J. Lin, *Biomaterials*, 2011, **32**, 4161; (*e*) F. Wang and X. G. Liu, *Chem. Soc. Rev.*, 2009, **38**, 976; (*f*) J. Wang, F. Wang, C. Wang, Z. Liu and X. G. Liu, *Angew. Chem., Int. Ed.*, 2011, **50**, 10369; (*g*) J. L. Liu, Y. Liu, Q. Liu, C. Y. Li, L. N. Sun and F. Y. Li, *J. Am. Chem. Soc.*, 2011, **133**, 15276.

9 (*a*) F. Auzel, *Chem. Rev.*, 2004, **104**, 139; (*b*) R. Scheps, *Prog. Quantum Electron.*, 1996, **20**, 271; (*c*) J. F. Suyver, A. Aebischer, D. Biner, P. Gerner, J. Grimm, S. Heer, K. W. Kramer, C. Reinhard and H. U. Gudel, *Opt. Mater.*, 2005, **27**, 1111.

10 (*a*) S. Sivakumar, F. C. J. M. van Veggel and M. Raudsepp, *J. Am. Chem. Soc.*, 2005, **127**, 12464; (*b*) F. van de Rijke, H. Zijlmans, S. Li, T. Vail, A. K. Raap, R. S. Niedbala and H. J. Tanke, *Nat. Biotechnol.*, 2001, **19**, 273; (*c*) G. S. Yi, H. C. Lu, S. Y. Zhao, G. Yue, W. J. Yang, D. P. Chen and L. H. Guo, *Nano Lett.*, 2004, **4**, 2191; (*d*) L. Y. Wang, R. X. Yan, Z. Y. Huo, L. Wang, J. H. Zeng, J. Bao, X. Wang, Q. Peng and Y. D. Li, *Angew. Chem., Int. Ed.*, 2005, **44**, 6054; (*e*) L. Wang and Y. Li, *Chem. Commun.*, 2006, **24**, 2557.

11 (*a*) S. Heer, K. Kompe, H. U. Gudel and M. Haase, *Adv. Mater.*, 2005, **16**, 2102; (*b*) J. H. Zeng, J. Su, Z. H. Li, R. X. Yan and Y. D. Li, *Adv. Mater.*, 2005, **17**, 2119.

12 (*a*) H. X. Mai, Y. W. Zhang, R. Si, Z. G. Yan, L. D. Sun, L. P. You and C. H. Yan, *J. Am. Chem. Soc.*, 2006, **128**, 6426; (*b*) J. C. Boyer, F. Vetrone, L. A. Cuccia and J. A. Capobianco, *J. Am. Chem. Soc.*, 2006, **128**, 7444; (*c*) J. C. Boyer, L. A. Cuccia and J. A. Capobianco, *Nano Lett.*, 2007, **7**, 847; (*d*) G. S. Yi and G. M. Chow, *Adv. Funct. Mater.*, 2006, **16**, 2324; (*e*) Y. Wei, F. Lu, X. Zhang and D. Chen, *Chem. Mater.*, 2006, **18**, 5733; (*f*) G. S. Yi and G. M. Chow, *Chem. Mater.*, 2007, **19**, 341.

13 Y. Sun, Y. Chen, L. Tian, Y. Yu, X. Kong, Q. Zeng, Y. Zhang and H. Zhang, *J. Lumin.*, 2008, **128**, 15.

14 S. Schietinger, L. D. S. Menezes and B. Lauritzen, *Nano Lett.*, 2009, **9**, 2477.

15 T. Y. Ohulchanskyy, H. E. Pudavar, E. J. Bergey, A. R. Oseroff and J. Morgan, *J. Am. Chem. Soc.*, 2003, **125**, 7860.

16 S. Z. Wang, R. M. Gao, F. M. Zhou and M. Selke, *J. Mater. Chem.*, 2004, **14**, 487.

17 X. D. Zhang, X. Jin, D. F. Wang, S. Z. Xiong, X. H. Geng and Y. Zhao, *Phys. Status Solidi C*, 2010, **7**, 1128.

18 D. K. Ma, S. M. Huang, Y. Y. Yu, Y. F. Xu and Y. Q. Dong, *J. Phys. Chem. C*, 2009, **113**, 8136.

19 C. Y. Cao, X. M. Zhang, M. L. Chen, W. P. Qin and J. S. Zhang, *J. Alloys Compd.*, 2010, **505**, 6.

20 X. Chen, W. J. Wang, X. Y. Chen, J. H. Bi, L. Wu, Z. H. Li and X. Z. Fu, *Mater. Lett.*, 2009, **63**, 1023.

21 L. Zhang and Y. J. Zhu, *J. Inorg. Mater.*, 2009, **24**, 553.

22 M. Estermann, L. B. Mclusker, C. Baerlocher, A. Merrouche and H. Kessler, *Nature*, 1991, **352**, 320.

23 Y. F. Chen, E. Johnson and X. G. Peng, *J. Am. Chem. Soc.*, 2007, **129**, 10937.

24 F. Zhao, M. Rutherford, S. Y. Grisham and X. G. Peng, *J. Am. Chem. Soc.*, 2009, **131**, 5350.

25 X. Jin, X. D. Zhang, Z. F. Lei, S. Z. Xiong, F. Song and Y. Zhao, *Acta Phys. Sin.*, 2008, **57**, 4580.

26 H. J. Liang, G. Y. Chen, L. Li, Y. Liu, F. Qin and Z. G. Zhang, *Opt. Commun.*, 2009, **282**, 3028.

